Architecture and Transport Properties of Multifilamentary MgB_2 Strands for MRI and Low AC Loss Applications

F. Wan, M. D. Sumption, M. A. Rindfleisch, M. J. Tomsic, and E. W. Collings

***Abstract*—Standard in-situ type MgB_2 strands manufactured by Hyper Tech Inc have 19 – 36 subelements, a monel outer sheath, and a Cu interfilamentary matrix. Typical transport J_cs of the strands are 2×10^5 A/cm^2 with *n*-values of 20 – 30 at 4.2 K and 5 T. This work introduces two new MgB_2 conductor designs. First, a new class of MgB_2 strand is designed for magnetic resonance imaging applications. This type has a higher Cu content designed to enhance protection of a magnet wound with it, and a larger diameter to increase the critical current. Second, a new class of low AC loss MgB_2 strand with high filament count and a high resistance matrix is discussed. Transport properties at 4.2 K and fields up to 10 T are reported. Optical techniques are used to study the macro- and micro-structures of these MgB_2 strands.**

***Index Terms*—MgB_2 strand, magnetic resonance imaging, low AC loss conductor, critical current density, strand design.**

I. Introduction

MAGNESIUM DIBORIDE is a promising superconductor for practical applications because of its transition temperature, T_c of 40 K [1] and low cost. One application is the magnet of a magnetic resonance imaging system (MRI). Compared to NbTi which has been widely utilized in MRI magnets, MgB_2 can greatly improve the stability of the MRI magnet due to the moderately high T_c [1]-[5]. In previous years, Hypertech Research Inc (HTR) and the Ohio State University have significantly improved the J_c and *n*-value of the MgB_2 wires. Typical J_c values of in-situ MgB_2 wires fabricated by HTR are 1×10^5 A/cm^2 at 4.2 K, 5 T and even 1×10^5 A/cm^2 at 4.2 K, 7 T [6]. Because the superconducting wire for an MRI magnet requires a much higher level of electrical stabilization and protection to operate in a helium free environment, we increased the volume fraction of Cu from 15% to 31% and decreased the subelement number from 36 to 18.

For practical superconducting applications, there is also interest in AC-loss reduction by the introduction of a resistive matrix and by twisting the multifilamentary strand [7]. However, the twisting process has the potential to introduce defects and suppress the J_c [8]-[13] and the *n*-value. But Yuan *et al*, reported that HTR has developed high filament MgB_2 strands which can tolerate substantial pre-reaction twisting; for example, powder-in-tube MgB_2 strands with 54 filaments and 10-100 mm twist pitch did not exhibit any J_c suppression at 4.2 K [13]. In this paper, we further decreased the twist pitch of MgB_2 strands to 5 mm and simultaneously increased the filament count to 114 in order to study the influence of the twisting process on the transport properties of multifilamentary MgB_2 strands.

On the path towards a high quality MgB_2, B powder is considered as a significant factor. One type of B powder used by HTR is fabricated by Specialty Materials Inc (SMI). The formation of SMI B powder is based on the reaction between BCl_3 and H_2 gases [14]. In addition, gaseous CH_4 is mixed with BCl_3 and H_2 for carbon doping [14]. Recently, HTR began to use the B powder from the Pavazyum (PVZ) Chemical Company. The PVZ B powder is formed by decomposing B_2H_6 gas [14]. This paper also describes the relative transport properties of powder-in-tube MgB_2 strands with SMI B and PVZ B.

Funding was provided by a NASA SBIR, a NIH SBIR, and the National Institute of Biomedical Imaging and Bioengineering, under R01EB018363.

F. Wan, M.D. Sumption and E. W. Collings are with the Center for Superconducting and Magnetic Materials (CSMM), Dept. of Materials Science and Engineering, The Ohio State University, Columbus, OH, USA. Corresponding author e-mails: wan.108@osu.edu.

M. A. Rindfleisch and M. J. Tomsic are with Hyper Tech Research, Columbus, OH, USA

II. Experimental

A. Samples

The multifilamentary MgB_2 strands used in this research (Table I and Table II) were manufactured and provided by HTR. All of the MgB_2 wires were heat-treated in a tube furnace and furnace-cooled. The soak temperature and heat treatment time were 675 ^{o}C and 60 min for standard and MRI wires; the MgB_2 low AC loss wires were heat treated at 650 ^{o}C/60 min.

B. Measurement of MgB_2 Wires

The transport J_c and *n*-value were measured in pool boiling liquid helium in transverse magnetic fields up to 10 T. The voltage criterion of J_c and *n*-value measurements was 1.0 μV/cm. The "standard" and MRI type wires were measured on ITER barrels [15]. For such a measurement, a 1 m-long MgB_2 wire was helically wrapped along a 9-turn groove in a Ti-Al-V alloy cylinder 30 mm in diameter and the ends of wire were soldered to the Cu caps of the alloy cylinder [6], [15], [16]. The separation of the voltage taps of each "standard" or MRI type wire was 500 mm. The 50 cm–long low AC loss wires (LAL 1-3) were measured in a short-sample holder. For low AC loss wire, the gauge length of voltage taps was 4 or 5 mm.

III. Results and Discussion

A. Transport J_c and n-Value of Standard MgB_2 Strands

The strand ST 1, ST 2, STT 1 and STT 2 were filled with the SMI B with 2.0% C doping and the SPVZ series wire

This is the author's version of an article that has been published in this journal. Changes were made to this version by the publisher prior to publication.
The final version of record is available at http://dx.doi.org/10.1109/TASC.2016.2632419

(SPVZ 1) was filled with 2.5% C doped PVZ B powder. The J_cs and n-values of the standard MgB_2 wires are shown in Fig. 1 and Fig. 2, respectively. It can be seen that the transport J_c and n-value at 5 T and 4.2 K of strand ST 1 are 1.77×10^5 A/cm^2 and 27, respectively, which are the best J_c and n-value of the ST-series wires. Fig. 3(a) shows the transverse cross sectional area of the sample ST 1.

TABLE I: THE STRUCTURE AND CHEMICAL COMPOSITION OF THE STANDARD AND MRI WIRE

Sample No.	Trace No.[a]	Filament No.	B Source[b]	T.P. (mm)[c]	Cu %[d]	Mg:B	C %[e]	MgB_2 %[f]	Dia. (mm)	H.T. (°C/min)
ST 1	3613	36	SMI	-	15	1:2	2.0	11.0	0.84	675/60
ST 2	3560	36	SMI	-	15	1:2	2.0	15.6	0.84	675/60
SPVZ 1	3497	36	PVZ	-	15	1.15:2	2.5	16.3	0.84	675/60
STT 1	3560	36	SMI	300	15	1:2	2.0	14.8	1.06	675/60
STT 2	3560	36	SMI	200	15	1:2	2.0	14.8	1.06	675/60
MRI 1	3648	19	SMI	-	31	1:2	2.0	8.7	0.84	675/60
MRI 2	3665	18	SMI	-	31	1:2	2.0	7.6	0.95	675/60
MRI 3	3614	18	SMI	-	31	1:2	2.0	7.5	0.84	675/60
MPVZ 1	3676	18	PVZ	-	31	1.15:2	2.5	10.0	0.95	675/60
MPVZ 2	3619	18	PVZ	-	31	1.15:2	2.5	11.1	0.95	675/60

TABLE II: THE STRUCTURE AND CHEMICAL COMPOSITION OF THE LOW AC LOSS WIRE

Sample No.	Trace No.[a]	Filament No.	B Source[b]	T.P. (mm)[c]	Mg:B	MgB_2 %[f]	d_{eff} (µm)[g]	Dia. (mm)	H.T. (°C/min)
LAL 1	3606	114	SMI	5, 30	1:2	11.2	20	0.60	650/60
LAL 2	3606	114	SMI	5, 50	1:2	13.9	30	0.80	650/60
LAL 3	3667	114	SMI	5, 30	1:2	12.3	33	1.00	650/60

[a] Sample number for internal purposes, [b] SMI: 2% C-doped SMI B. PVZ: 2.5 % C-doped PVZ B. [c] Twist pitch of MgB_2 wire, [d] Percentage of Cu in the MgB_2 strand, [e] Carbon doping level, [f] Powder percentage of the MgB_2 in the whole strand, [g] Effective filament diameter, **Note:** All MgB_2 standard and MRI wires used Nb barrier, monel outer sheath, Cu central filament, and Cu interfilament, while MgB_2 low AC loss wire used Nb barrier, Cu10Ni subelement sheath, Cu30Ni outer sheath, Cu10Ni central filament, and Cu interfilament.

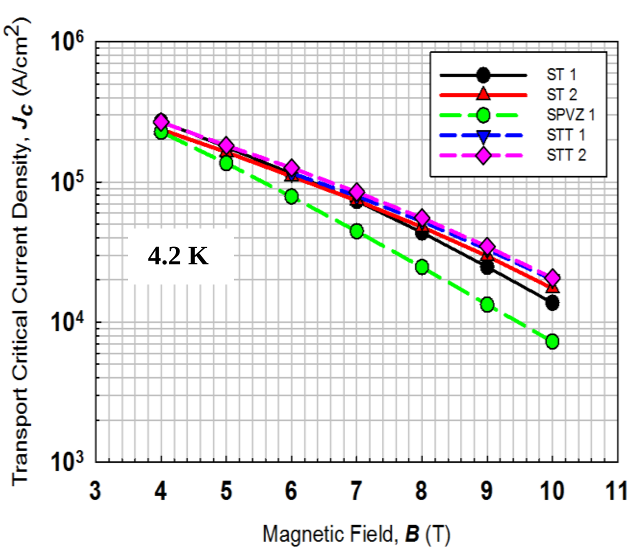

Fig. 1: Field dependence of the transport J_cs of the standard MgB_2 wires.

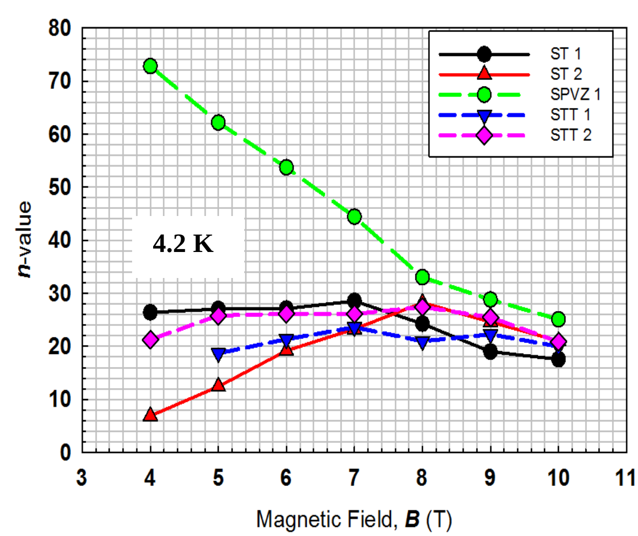

Fig. 2: Field dependence of the n-values of the standard MgB_2 wires.

Compared to the ST series wires, the SPVZ series strand has slightly lower transport J_cs at all measured magnetic fields. For multifilamentary standard MgB_2 wires, the sample SPVZ 1(Fig. 3(b)) had the best *n*-value of all standard strands at 4.2 K in all fields of 4 T to 10 T, although further measurements and statistical analysis would be needed to see if any general conclusion can be made on this point. The ratio of Mg to B for SPVZ series wire is larger than 1:2, which possibly makes the transport properties of the SPVZ series wire different from the ST series wires. The ratio of Mg to B for SPVZ series wire was chosen to be 1.15:2 in order to optimize the transport J_c of the MgB_2 wires filled with PVZ B according to previous (unreported) studies.

The STT series wires represent the standard MgB_2 wires processed with twisting. Sample STT 1 with 300 mm twist pitch and STT 2 with 200 mm twist pitch are the twisted versions of sample ST 2. The strand STT 2 attained the best J_c at 6 T and 4.2 K (1.26×10^5 A/cm^2) of all the standard MgB_2 wires.

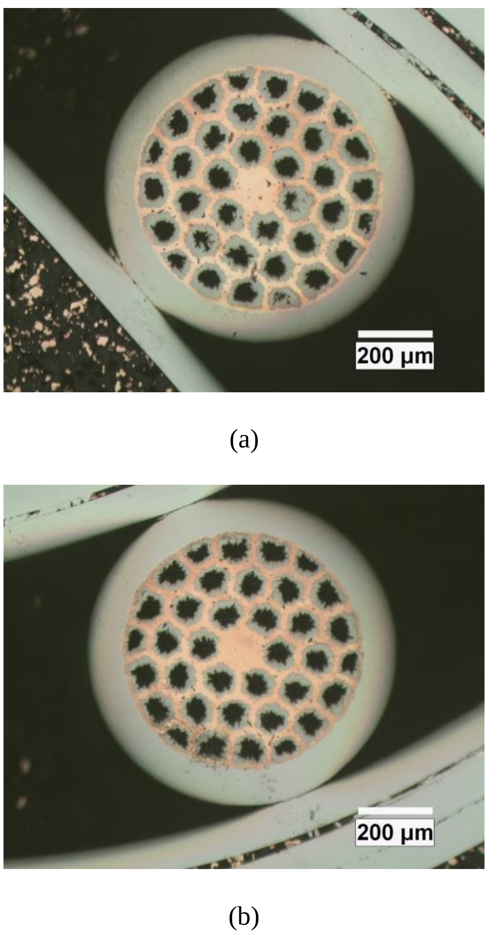

Fig. 3. Optical image of sample (a) ST 1 and (b) SPVZ 1.

B. Transport J_c and n-Value of MRI MgB_2 Barrels

A series of strands for MRI was studied; the J_cs and *n*-values are shown in Fig. 4 and Fig. 5, respectively. The strand MRI 1 attained the best J_c (2.2×10^5 A/cm^2) at 5 T and 4.2 K, of all the MgB_2 wires wound with MRI-type strand. Fig. 6(a) shows the transverse cross sectional area of the sample MRI 2. MPVZ series wires (MPVZ 1 and MPVZ 2), which are the MRI MgB_2 wire based on PVZ B powder, exhibited slightly lower transport J_c than the MRI series wires based on the SMI B in the fields of 7 T to 10 T. But the sample MPVZ 1 (Fig. 6(b)) attained the higher *n*-values than the MRI series strands did in fields of 5 T to 9 T and the sample MPVZ 2 attained the best *n*-value at 5 T (74) of all the MRI-type MgB_2 wires.

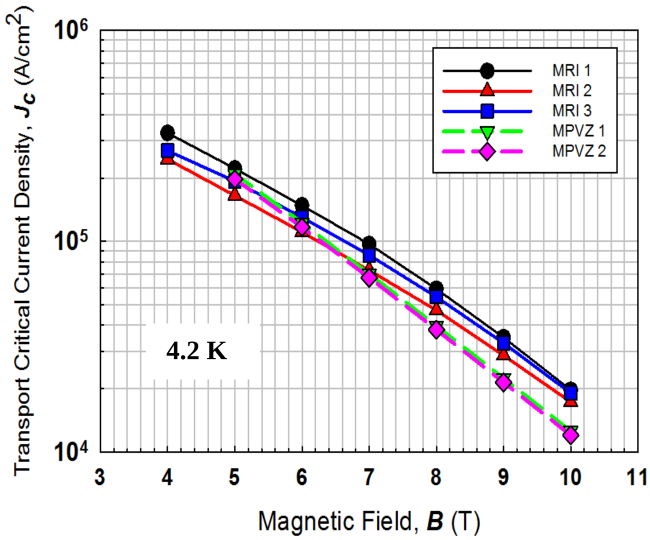

Fig. 4. The transport J_c*s* of MgB_2 wires for MRI versus magnetic field.

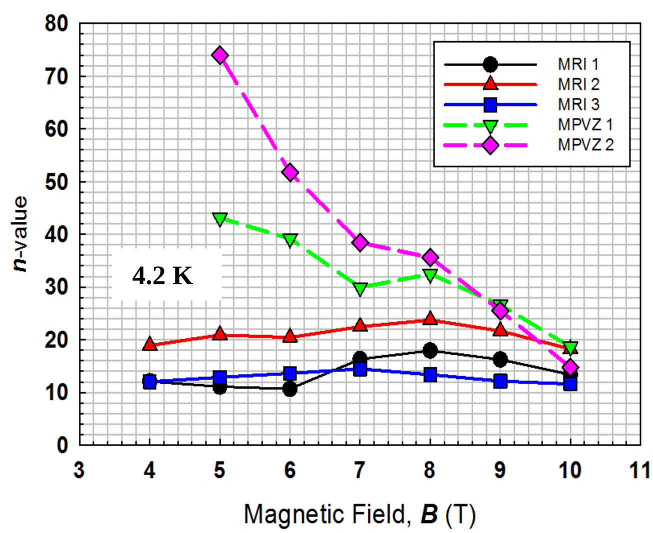

Fig. 5. *n*-values of MgB_2 wires for MRI versus magnetic field.

C. MgB_2 Low AC Loss Wire

Fig. 7 shows the cross sectional area of the sample LAL 1. The transport J_cs and *n*-values of MgB_2 low AC loss wires are shown in Fig. 8 and Fig. 9, respectively. The strands had filament diameters of 20-33 µm, and resistive matrices, as described in Table II. Although not presented here, the Cu-Ni alloys used for these conductors had much lower magnetic signatures than previous strands with monel outer shells. The twist pitch of the LAL series strands ranges from 5 mm to infinity (untwisted). The LAL series strands exhibited no twisting-induced suppression in transport J_cs at all measured fields. Some strands with a 5 mm twist pitch attained the same or even slightly higher transport J_cs than the untwisted strands. At 4.2 K and 7 T, all the wires have *n*-values larger than 20 except sample LAL 1 with 5 mm twist pitch. However, considerable scatter in the *n*-values of the wires is seen. In any case, the transport J_c of the strands was not degraded by twisting down to 5 mm.

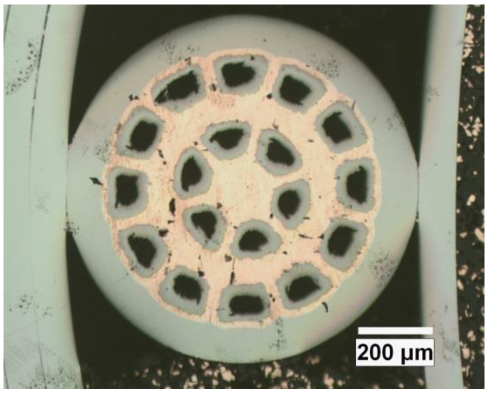

(a)

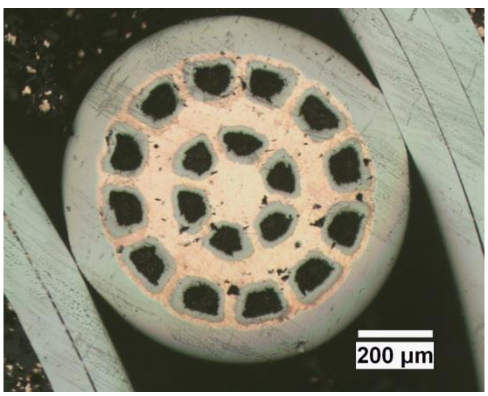

(b)

Fig. 6. Optical image of (a) MRI 2 and (b) MPVZ 1.

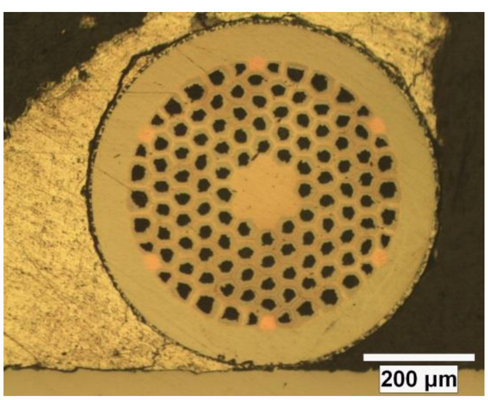

Fig. 7. Optical image of the transverse cross sectional area of the sample LAL 1 with 5 mm twist pitch.

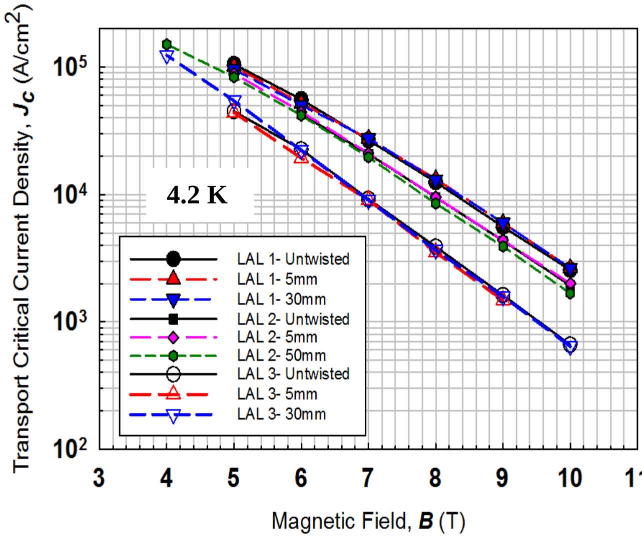

Fig. 8. Field dependence of transport J_c for low AC loss wires

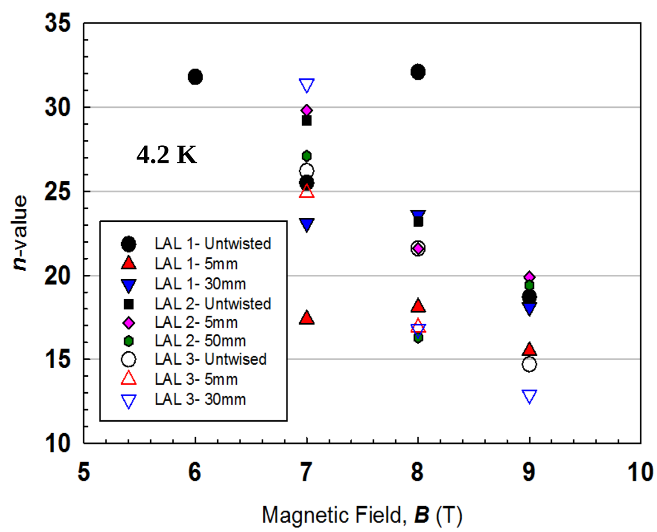

Fig. 9. Field dependence of *n*-value for low AC loss wires.

IV. Conclusion

A series of in-situ powder-in-tube multifilamentary MgB_2 strands manufactured for general applications and MRI have been studied. The best transport J_c at 4.2 K and 5 T was 2.2 × 10^5 A/cm^2, obtained by MRI 1 and the best *n*-value was 74 at 4.2 K and 5 T obtained by MPVZ 2. MRI MgB_2 strands have attained transport J_cs and *n*-values similar to those of the standard MgB_2 wire and higher Cu content enable the MRI MgB_2 strands to have improved quench protection (or lead to magnets with better quench protection). It seems that the PVZ B is as good as the SMI B for multifilamentary MgB_2 strands. A new class of low loss MgB_2 strands has been demonstrated which has a high filament count, and is capable of very low twist pitch value, with no J_c degradation.

REFERENCES

[1] J. Nagamatsu, N. Nakagawa, T. Muranaka, Y.Zenitani, and J. Akimitsu, "Superconductivity at 39 K in magnesium diboride," *Nature*, vol. 410, pp. 63-65, 2001.

[2] Jiayin Ling, John Voccio, Seungyong Hahn, Youngjae Kim, Jungbin Song, Juan Bascuñán and Yukikazu Iwasa, "Development of a 0.5-T/240-mm MgB_2 MRI Magnet: Assembly Design and Module Coils," *IEEE Trans*, *Appl*. *Supercond*., vol. 24, no. 3, pp. 1-5, Jun 2014.

[3] M. Tomsic, M. Rindfleisch, J. Yue, K. McFadden, and J. Phillips, "Overview of MgB_2 superconductor applications," *Int. J. Appl. Ceram. Technol*., vol 4, no. 3, pp. 250-259, 2007.

[4] A, Stenvall, I. Hiltunen, A. Korpela, J. Lehtonen, R. Mikkonen, J. Viljamaa, and G. Grasso, "A checklist for designers of cryogen-free MgB_2 coils," *Supercond. Sci. Technol*., vol. 20, no. 4, pp. 386-391, Apr. 2007.

[5] M. Razeti, S. Angius, L. Bertora, D. Damiani, R. Marabotto, M. Modica, D. Nardelli, M. Perrella, and M. Tassisto, "Construction and operation of cryogen free MgB_2 magnets for open MRI systems," *IEEE Trans, Appl. Supercond*., vol. 18, no. 2, pp. 882-886, June. 2008.

[6] G. Z. Li, K. M. Reddy, J. B. Zwayer, M. A. Kuldell, M. A. Susner, Y. Yang, M. D. Sumption, J. J. Yue, M. A. Rindfleisch, M. J. Tomsic, C. J. Thong, and E. W. Collings, "Critical current density and current transfer length of multifilamentary MgB_2 strands of various design," *IEEE Trans, Appl. Supercond*, vol. 23, no. 3, pp. 6200204, June. 2013.

[7] Henning Taxt, Niklas Magnusson, Magne Runde, and Silvia Brisigotti, "AC loss measurements on multi-filamentary MgB_2 wires with non-magnetic sheath materials," *IEEE Trans, Appl. Supercond*, vol. 23, no. 3, pp. 8200204, June. 2013.

[8] P Kováč, I Hušek, T Melišek, E Martínez and M Dhalle, "Properties of doped ex and in situ MgB_2 multi-filament superconductors," *Supercond. Sci. Technol*., vol. 19, no. 10, pp. 1076-1082, Oct. 2006.

[9] A Malagoli, C Bernini, V Braccini, C Fanciulli, G Romano and M Vignolo, "Fabrication and superconducting properties of multifilamentary MgB_2 conductors for AC purposes: twisted tapes and wires with very thin filaments," *Supercond. Sci. Technol*., vol. 22, no. 10, pp. 105017, Oct. 2009.

[10] P Kováč, I Hušek, T Melišek, L Kopera and M Reissner, "Stainless steel reinforced multi-core MgB_2 wire subjected to variable deformations, heat treatments and mechanical stressing," *Supercond. Sci. Technol*., vol. 23, no. 6, pp. 065010, June. 2010.

[11] P Kováč, I Hušek, T Melišek, and L Kopera, "Filamentary MgB_2 wires twisted before and after heat treatment," *Supercond. Sci. Technol*., vol. 24, no. 11, pp. 115006, Nov. 2011.

[12] P Kováč, L Kopera, T Melišek, M Rindfleisch, W Haessler and I Hušek, "Behaviour of filamentary MgB_2 wires subjected to tensile stress at 4.2 K," *Supercond. Sci Technol*., vol. 26, no. 10, pp. 105028, 2013.

[13] Y. Yang, G. Z. Li, M. A. Susner, M. D. Sumption, M. A. Rindfleisch, M. J. Tomsic, E. W. Collings, "Influence of twisting and bending on the J_c and *n*-value of multifilamentary MgB_2 strands," *Phys. C*, vol. 519, pp. 118-123, 2015.

[14] E. W. Collings, G. Z. Li, M. D. Sumption, and M. A. Susner, "Chapter 4f: Development and properties of advanced internal magnesium infiltration (AIMI) processed MgB_2 wires," in *MgB_2 Superconducting Wires Basics and Applications*, vol. 2, Singapore: World Scientific, 2016, pp. 341-388.

[15] M. D. Sumption and E. W. Collings, "Stability and instability in high performance (metastable) composite strands during I-V measurement", *Physica C*, vol. 401, no. 1-4, pp. 66-74, 2004.

[16] A. Nijhuis, W. A. J. Wessel, H. G. Knoopers, Y. Ilyin, A. della Corte, and H. H. J. ten Kate, "Compressive pre-strain in Nb_3Sn strand by steel tube and effect on the critical current measured on standard ITER barrel," *IEEE Trans. Appl. Supercond*, vol. 15, no. 2, pp. 3466-3469, June. 2005.